Available online at www.sciencedirect.com

ScienceDirect

Energy Procedia 49 (2014) 1147 – 1156

Energy Procedia

SolarPACES 2013

Simulation of a hybrid solar gas-turbine cycle with storage integration

B. Grange[a], C. Dalet[a], Q. Falcoz[a], F. Siros[b], A. Ferrière[a]

[a]*CNRS-PROMES, 7 rue du Four Solaire, 66120 Font-Romeu, France*
[b]*EDF R&D, 1 Avenue du Général de Gaulle, 92140 Clamart, France*

Abstract

The interest for hybrid solar gas-turbine systems (HSGT) in solar tower plant technologies is growing This is due to the high conversion efficiency and to the low water consumption that are achieved when a combined cycle is implemented. This paper presents a simulation tool which is dedicated to the performance analysis of the top cycle featuring a thermal energy storage unit (TES). The influence of the TES operating conditions on the power plant production is highlighted.. A major advantage of the storage is to stabilize the air temperature at the combustion chamber inlet in order to keep the operating conditions of the combustion chamber close to the design point. This work establishes that a higher and more stable electrical generation is achieved through this concept. According to the storage capacity, the TES unit increases the daily average solar share of the power plant. This study is conducted within the framework of the French PEGASE project (Production of Electricity from Gas and Solar Energy) which aims at setting up and testing at THEMIS site (France) a demonstration plant based on HSGT technology.

Selection and peer review by the scientific conference committee of SolarPACES 2013 under responsibility of PSE AG.
Final manuscript published as received without editorial corrections.
Keywords: CSP, Thermodynamic Cycle Modelling; Gas Turbine ; Thermal Energy Storage

1. Introduction

Most solar thermal power plants are able to incorporate large capacity thermal energy storage (TES) units. TES increases the capacity factor and allows for more dispatchable power [1]. It also offers ancillary services to the grid. This makes concentrated solar power (CSP) a very attractive electricity generation technology compared to other renewable electricity generation systems. Therefore TES provides a high potential for the penetration of CSP in the existing grid [2].

A recent review on the state of the art of high temperature TES for power generation focusing on concepts, materials and simulation assessed the added value of TES technology in CSP systems [3]. However very few case

Selection and peer review by the scientific conference committee of SolarPACES 2013 under responsibility of PSE AG.
Final manuscript published as received without editorial corrections.
doi:10.1016/j.egypro.2014.03.124

studies featuring TES in CSP systems have been investigated so far. To achieve a better understanding of the behavior of TES coupled with CSP systems, a comprehensive analysis should be undertaken [4]. The present work intends to contribute to this analysis.

Camacho et al. [5, 6] proposed advanced control techniques applied to a global CSP system simulation in order to address the issue of intermittent solar radiation. But these techniques generally do not consider TES and focus on the heat transfer fluid flow-rate as an actuator to set the temperature at the outlet of the solar collector [7].

Most of the existing simulation works are dedicated to the parabolic trough technology. Experiments with molten salt tower technology at Themis (France, 1986), Solar Two (USA, 2000), and more recently at Gemasolar (Spain, 2010) have demonstrated the added value created by molten salt TES in the case of a solar tower plant [8]. But no system analysis based on simulation work has been published so far.

A few global simulation tools allow modeling various solar power plant technologies such as parabolic trough, molten salt tower or HSGT. As an example, a CSP performance model was recently developed by NREL and Sandia National Laboratory and it was implemented in SAM (System Advisor Model) [9]**.** NREL has also,developed a "generic solar system" performance model for use in SAM. In this tool the TES component is modeled using a simple energy-balance approach. Giuliano et al. [10] assessed the performance of solar thermal power plants with TES featuring a hybrid solar operation strategy on an annual basis. Various CSP technologies (integrated solar combined cycle, parabolic trough, molten salt tower, CO_2-tower, particle receiver tower with combined cycle) were considered with different sizes of solar field and different storage capacities. The commercial software Ebsilon was used for simulating the operation of the plant. The results showed that the potential to reduce the CO_2 emission is high for a solar thermal plant with large storage capacity when it is operated in base-load.

A dynamic modeling of the complete system integrating a TES unit is necessary to better understand how the storage interacts with the other components of the system. The heat transfer fluid (HTF) flow-rate through the storage is an interesting additional operating parameter. This parameter allows a better control of the air temperature at the outlet of the solar receiver. The stabilization of this temperature is essential in the case of a hybrid solar-gas turbine power plant. Most of the conventional gas turbine power plants are not suited for the hybridization with an intermittent energy source [11]. The adaptation of the combustion chamber to a large range of fuel / air ratio (FAR) is a major issue of the hybridization. The solar hybridization of a gas-turbine is therefore a technical challenge.

This paper deals with the development of a global simulation tool dedicated to the innovative technology of hybrid solar-gas turbine power plant integrating a thermal energy storage system. The influence of the TES operating conditions on the performance of the combustion chamber -and thus on the power plant production- is studied. This study takes place within the framework of the French PEGASE project (Production of Electricity from Gas and Solar Energy) which aims at setting up and testing at THEMIS site (France) a demonstration plant based on HSGT technology [12].

Nomenclature

c_p	specific heat (J/kg.K)
H	enthalpy (J/kg)
m	mass (kg)
P	power (W)
S	area (m^2)
t	time (s)
T	temperature (K)
η	efficiency (-)
τ_{sol}	solar share

2. Operation modes

The hybrid solar – gas turbine power plant which is considered here features a solar field and a tower. The power block is located at the top of the tower. It is made up of a compressor, a pressurized air solar receiver, a combustion

chamber fed with natural gas (CH_4) and an expander coupled to an electrical power generator. In this system, pressurized air is the HTF and is the working fluid as well. A sensible heat storage unit is integrated in the air streamline parallel to the solar receiver (Figure 1).

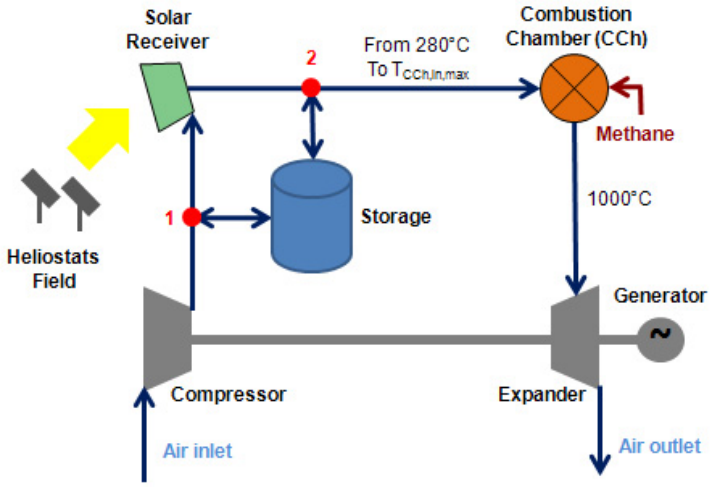

Fig. 1. Schematic of a solar hybrid gas-turbine power plant with storage.

The operating mode of the storage (idle, charging, discharging) is selected by comparing the air temperature at the solar receiver outlet with the maximum temperature at the combustion chamber inlet ($T_{CCh,in,max}$) and by considering the storage status. The storage is empty/full when the average temperature reaches 110 % of the compressor outlet temperature/ $T_{CCh,in,max}$ respectively. The air mass flow-rate in the compressor and in the combustion chamber remains constant in all operating modes. The air flow circulates through the storage unit from point 1 to point 2 (or from 2 to 1) when the storage is discharged (charged, respectively). In charging mode, a blower is used to push the air through the storage. The air mass flow-rate through the solar receiver is increased accordingly. A high pressure drop through the solar receiver decreases the turbine efficiency. Therefore a maximal value of the air flow-rate through the solar receiver is considered. In discharging mode, the receiver is partially or fully by-passed, according to the solar irradiation and to the temperature of the storage.

2.1. Solar receiver only operation mode

TES is idle in this mode. The air mass flow-rate in the solar receiver is at design value. Two situations are considered:

- The storage is empty and the solar resource is insufficient to achieve the air temperature $T_{CCh,in,max}$ at the outlet of the receiver.
- The storage is full and the air temperature $T_{CCh,in,max}$ is achieved at the outlet of the receiver. The solar field might be partly defocused in order to keep the air temperature at $T_{CCh,in,max}$.

2.2. Storage charging

The storage is not full. The mass flow-rate through the solar receiver is increased in order to keep $T_{CCh,in,max}$ at the outlet. The additional mass flow-rate through the receiver is directed to the storage (point 2 on Figure 1) and is sent back into the solar receiver downstream the storage unit (point 1 on Figure 1).

2.3. Storage discharging

When the storage average temperature is higher than the solar receiver outlet temperature, a part of the mass flow-rate at the outlet of the compressor (point 1 on Figure 1) is directed to the storage.

3. Modelling

The key parameters that determine the power plant performances are the electrical production, the cycle efficiency η_{th} and the solar share τ_{sol}. The cycle efficiency is the mechanical work delivered by the cycle over the heat provided to the fluid. The mechanical work delivered by the cycle is the work provided by the expander minus the work consumed by the compressor. The heat provided to the fluid is the sum of the enthalpy gained in the solar receiver ΔH_{receiv}, in the combustion chamber ΔH_{CCh} and in the storage $\Delta H_{storage}$ (positive/negative under discharging/charging respectively).

$$\eta_{th} = \frac{\Delta H_{comp} - \Delta H_{exp}}{\Delta H_{receiv} + \Delta H_{storage} + \Delta H_{CCh}} \quad (1)$$

The solar share is the solar contribution to the heat provided to the fluid. It comes from both the solar receiver and from the storage. Consequently, the solar fraction is expressed as,

$$\tau_{sol} = \frac{\Delta H_{receiv} + \Delta H_{storage}}{\Delta H_{receiv} + \Delta H_{storage} + \Delta H_{ChC}} \quad (2)$$

The outlet parameters of the model are obtained using enthalpy balances between the inlet and the outlet of each component. The efficiency of a component is the ratio between the actual enthalpy variation of the fluid through the component and the one in the ideal case (without any losses). This efficiency is a function of the operating point and of the component design parameters. The model is quasi-static: it solves, at each time step, the energy balances as a function of the operating conditions starting from the thermodynamic equilibrium determined at the previous time step. The solar flux impinging on the receiver (P_{SF}) is calculated from the efficiency matrix of the solar field η_{SF} and from the DNI (Direct Normal Irradiance):

$$P_{SF} = \eta_{SF} \times DNI \times S_{mir} \quad (3)$$

The heat transferred to the fluid in the solar receiver (ΔH_{air}) is determined from the solar flux intercepted by the solar receiver P_{SF} and from the receiver efficiency η_{SR} (Equation 4). The receiver efficiency η_{SR} is evaluated by a model of cavity receiver designed for an outlet air temperature of 750°C [13] using experimental results for the performance of the absorber [14]. It depends on the inlet air temperature in the solar receiver and on the solar incident power.

$$\Delta H_{air} = \eta_{SR} P_{SF} \quad (4)$$

The isentropic efficiency is used to characterize the compressor and the expander. The combustion efficiency is defined as the ratio between the actual amount of heat released by the reaction and the ideal one. The ideal enthalpy of reaction is equal to the heat produced when the reaction is complete. It is calculated with the low heat value (LHV). The actual amount of heat released by the reaction is determined assuming that:

- the combustion is adiabatic (all the heat released by the reaction is used to raise the temperature of the products), which means that the enthalpy variation of the species between the inlet and the outlet of the combustion chamber is equal to zero,
- the stoichiometric coefficients of all the species which participate to the reaction, including the nitrogen, are taken into account.

The heat storage implemented in the power plant is based on sensible heat technology. In order to remain independent from a specific storage design, the storage unit is characterized by a sensible efficiency η_s which is the ratio between the enthalpy variation of the actual storage and an ideal storage unit. The sensible efficiency is introduced by Kay and London [15]: it depends on the operating conditions and on the design parameters of the storage. In the model, the sensible efficiency is an input parameter and is equal to 0.99. The ideal storage unit features an infinite transfer area. The enthalpy variation is determined for the actual storage by using Equation 5.

$$\Delta H_{storage,actual} = \eta_s \Delta H_{storage,ideal} \tag{5}$$

In the case of an ideal storage (η_s=1), the temperature of the storage material is assumed to be uniform through the storage. This temperature is called the mean temperature of the storage and is written $T_{storage,mean}$. Since the ideal storage has an infinite transfer area, the air temperature at the outlet of the storage $T_{storage,out}$ is equal to the storage mean temperature. Consequently, the enthalpy variation through an ideal storage can be easily calculated by using the following equations:

$$\begin{cases} T_{storage,out}(t) = T_{storage,mean}(t) \\ (m \cdot c_p)_{storage}\left[T_{storage,mean}(t) - T_{storage,mean}(t - \Delta t)\right] = \Delta H_{storage}\Delta t \end{cases} \tag{6}$$

The term $(m.Cp)_{storage}$ is the heat capacity of the storage material. This parameter is an input of the model.

The TES capacity is calculated for a nominal air mass flow-rate of 8 kg/s and a characteristic discharge time of 5 hours. A loop integrating Equations 5 and 6 determines the value of $(m.Cp)_{storage}$ for which the air at the storage outlet reaches a temperature of 330°C after 5 working hours. The value of $(m.Cp)_{storage}$ corresponding to our case-study is 65,000 kJ/K.

4. Results

The design operating conditions of the plant are reported in Table 1. In order to keep within the range of solar receiver outlet temperature and to maximize the solar share, a thermal energy storage unit is integrated in the system. The maximum value of the solar receiver outlet temperature is set to 750°C, which is also the maximum temperature allowed at the combustion chamber inlet $T_{CCh,in,max}$.

The operation of the solar hybrid power plant is simulated with the model over 14 working hours, on the basis of one day featuring a clear sky –from 6 a.m. to 3 p.m.- followed by a cloudy afternoon and evening from 3 p.m. to 8 p.m. (see Figure 2). The operation strategy consists in maximizing both the electricity generation and the conversion rate of the available solar resource. This simulated operation allows studying a storage charging mode followed by a storage discharging mode.

Figure 3a shows the evolution of the breakdown of solar and fossil contributions to the power generation. Figure 3b plots the air mass flow-rate in the main components: storage unit, solar receiver, combustion chamber. The operating modes defined in section 2 are distinguished in Figure 3. In the early morning, the DNI is equal to zero and the storage is empty. The storage is idle and the plant operates in the fossil-only mode. From 6:30 a.m. to 7:30 a.m., the solar contribution to the heat provided to the fluid increases, while the fossil contribution decreases accordingly. During this period, the DNI is not high enough to reach 750°C at the solar receiver outlet. Consequently the storage remains idle. The air mass flow-rate in the receiver is constant.

Table 1. Design data for the operation of the solar hybrid power plant.

	Atmospheric pressure [bar]	0.85
	Nominal mass flow-rate [kg/s]	8
	Pressure losses coefficient within pipes	1
Filter	Pressure losses coefficient	0.99
Compressor	Compression rate	7.9
	Isentropic efficiency	0.85
Solar receiver	Pressure losses coefficient	0.97
	Maximal mass flow-rate through the receiver [kg/s]	15
	Maximal temperature at the outlet [°C]	750
Solar field	Number of heliostat	200
	Surface [m²]	54
Storage	Initial temperature [°C]	200
	Nominal mass flow-rate [kg/s]	8
	Discharge time at the nominal mass flow-rate [h]	5
	Pressure losses coefficient	0.99
	Efficiency	0.99
Combustion chamber	Range of inlet temperature [°C]	420 - 750
	Target temperature at the outlet [°C]	1000
	Pressure losses coefficient	0.96
	Combustion efficiency	1
	Fuel temperature at the inlet [°C]	25
	Type of carburant	Methane
	Range of FAR	0.02 - 0.04
Expander	Isentropic efficiency	0.89
Chimney	Pressure losses coefficient	0.98
	Pressure at the outlet [bar]	0.85
Gas turbine shaft	Losses shaft /compressor	0
	Losses shaft / turbine	0

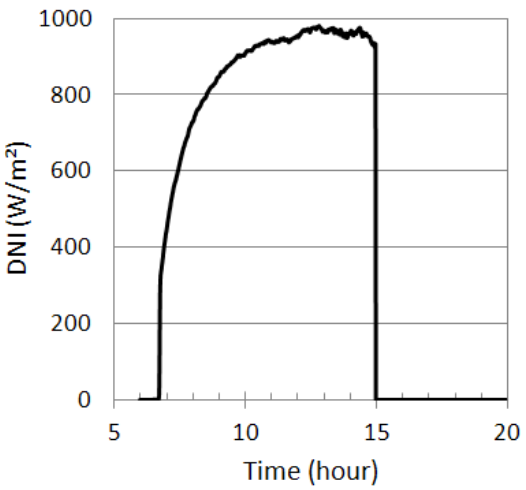

Fig. 2. DNI variation.

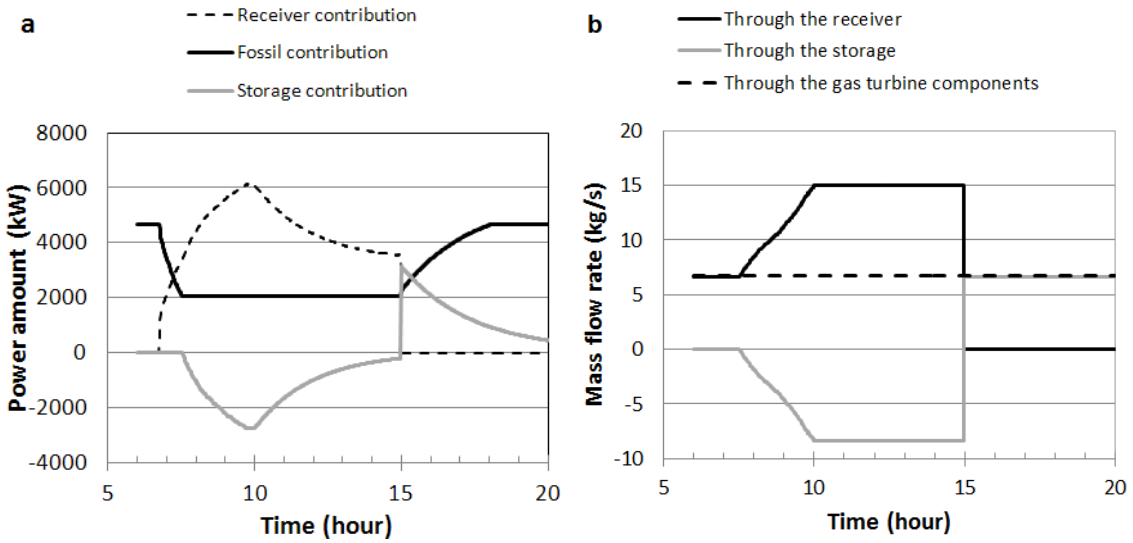

Fig. 3. (a) solar and fossil contribution provided to the fluid; (b) air mass flow rate through the power plant components.

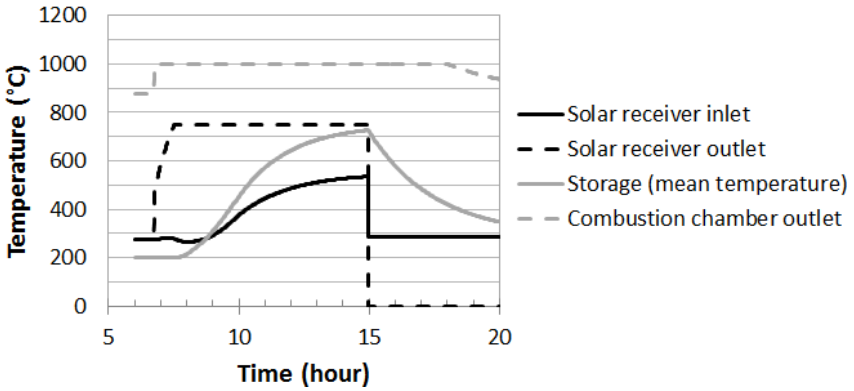

Fig. 4. Temperature at the outlet of the power plant components.

At 7:30 a.m. the solar receiver outlet temperature reaches 750°C. The storage charging mode starts. The recirculation of air increases the mass flow-rate in the receiver and the solar receiver outlet temperature is stabilized at 750°C. Symmetrically, the mass flow-rate through the storage increases with the same slope (negative value in charging mode) and the storage contribution is negative (heat is stored, it is not transmitted to the working air).

At 10 a.m. the mass flow-rate through the storage reaches its maximum value, it cannot be increased any more. Therefore the air mass flow-rate through the receiver is stabilized as well. When the DNI slightly increases, the number of operating heliostats must be decreased to keep the solar receiver outlet temperature at 750°C. From 10 a.m. to 3 p.m. the mass flow-rate through the storage and the air temperature at the storage inlet remain constant while the average temperature of the storage material increases (Figure 4). Less heat is transferred from the air to the storage material.

From 3 p.m. to 6 p.m., there is no sun and the storage discharging keeps the air temperature at the combustion chamber inlet higher than 420°C. Over 420°C, the FAR allows the combustion chamber to heat the air at the target temperature of 1000 °C (Figure 4). After 6 p.m., the heat released by the TES is too low and the upper limit of the

FAR is reached. Therefore the temperature at the outlet of the combustion chamber drops below 1000°C. The expander efficiency drops down consequently.

To show the effect of the storage integration on the power plant performances, a hybrid power plant without storage is considered and the operation is simulated using the same model. This plant gives the priority to the electrical production over the solar share. The simulated results in both cases (with and without storage capability) are compared. Figure 5 shows the evolution of the cycle efficiency for both cases.

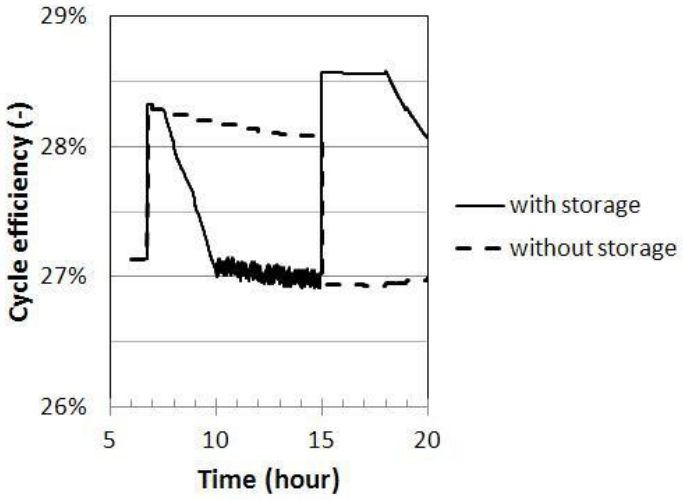

Fig. 5. Cycle efficiency of the hybrid power plant with storage and without storage

Before 6:30 a.m. there is no sun and the storage is empty. From 6:30 a.m. to 7:30 a.m. the solar resource remains low, the storage charging is not started, the cycle efficiency is 28.3 % for both plants.

Then the DNI is high enough to start the storage charging. The mass flow-rate in the receiver increases, the cycle efficiency of the plant with storage decreases from 28.3% to 27.1%. This is caused by the lower pressure at the expander inlet.

At 10 a.m., the maximum mass flow-rate allowed in the solar receiver is reached.

After 3 p.m. the storage discharge operating mode is started, the additional pressure drop due to the higher mass flow-rate in the solar receiver disappears. The cycle efficiency jumps from 27 % to 28.6 % at the beginning of the storage discharging. At 6 p.m., the thermodynamic efficiency decreases due to a lower air temperature at the storage outlet.

The integration of the storage leads not only to a stabilization of the air temperature at 750°C at the combustion chamber inlet, but also to an increase of the solar contribution (the stored energy is solar energy). Indeed with the integration of the TES, the solar share increases from 37.5 % to 44.7 %. Due to the stabilization of the expander inlet temperature at 1000°C, the hybrid power plant with storage produces 5.4 % more electricity than the same plant without storage. The amount of fuel consumed by the power plant with storage is 6.7 % lower than the one of the power plant without storage. This lower fuel consumption induces an electrical production per ton of consumed fuel 13 % higher than the one without storage (6.16 MWh/t_{fuel} and 6.96 MWh/t_{fuel} for the plant without and with storage, respectively). Note that if the operating strategy of the hybrid power plant without storage is to favor the solar share over the electrical production, the electrical production per ton of consumed fuel would be slightly higher than the one with storage but the electrical production would be much lower.

The maximum flow-rate allowed in the solar receiver is a critical parameter not only for optimizing the solar share, but also for designing the size of the storage. Figure 6 shows the evolution of the average temperature of the storage and the air temperature at the combustion chamber inlet for two values of the maximum flow-rate in the solar receiver (10 kg/s and 15 kg/s). The gas turbine components still operate at constant mass flow-rate. The

decrease of the maximum flow-rate in the solar receiver leads to a decrease of the storage average temperature: after 7h30 of storage charging, the storage average temperature is 727°C when the maximum flow-rate is 15 kg/s, while it is 618°C for a maximum mass flow-rate of 10 kg/s. Thus the solar fraction decreases from 44.7 % to 42.6 % and the electrical production per ton of consumed fuel is equal to 6.76 MWh/t_{fuel}.

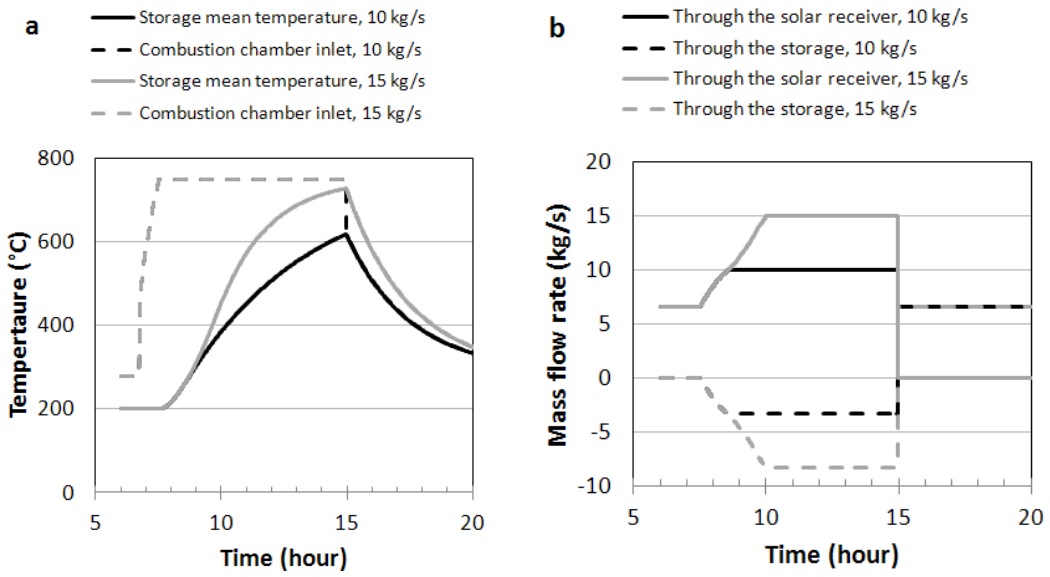

Fig. 6. Influences of the maximal mass flow-rate allowed in the receiver on (a) the outlet temperature of the power plants components; (b) the mass flow-rate through the storage and through the receiver

5. Conclusion

One of the main advantages of the storage integration is to stabilize the air temperature at the combustion chamber inlet in order to keep within the operating conditions range defined by the fuel-air ratio. This ensures higher and more stable electrical production. Moreover, the storage discharging during a cloudy period guarantees a positive solar share over a longer time. This also leads to a better use of the solar field. However, the chosen architecture leads to a lower pressure at the expander inlet during the storage charging mode which implies a slight decrease of the electrical production.

The maximum mass flow-rate allowed in the solar receiver is a critical parameter to size the storage unit. The higher it is, the faster the storage charging is. An optimization of the maximum mass flow-rate in the receiver must be performed. It is a function of the pressure drop in the receiver which is directly linked to the electrical production, for the given storage size and for the nominal DNI during the storage charging phase.

The model developed can be prone to some improvements, such as an evolution of the storage efficiency as a function of the operating conditions. In that case, a specific design of the storage should be considered, which allows to study a more realistic power plant. Finally different architectures of hybrid power plant with TES integration must be compared in order to maximize the power plant efficiency.

References

[1] Medrano M et al. State of the art on high-temperature thermal energy storage for power generation. Part 2: Case studies. Renewable and Sustainable Energy Reviews, 2010, Vol. 14, p. 56-72.

[2] Denholm P and Mehos M. Enabling Greater Penetration of Solar Power via the Use of CSP with Thermal Energy Storage. Technical Report NREL/TP-6A20-52978, November 2011.

[3] Gil A. et al. State of the art on high temperature thermal energy storage for power generation. Part 1--Concepts, materials and modellization. Renewable and Sustainable Energy Reviews, 2010, Vol. 14, p. 31-55.
[4] Powell KM, Edgar TF. Modeling and control of a solar thermal power plant with thermal energy storage. Chemical Engineering Science, 2012, Vol. 71, p. 138-145.
[5] Camacho EF, Rubio FR, Berenguel M, Valenzuela L. A survey on control schemes for distributed solar collector fields. Part I: Modeling and basic control approaches. Solar Energy, 2007, Vol. 81, p. 1240-1251.
[6] Camacho EF, Rubio FR, Berenguel M, Valenzuela L. A survey on control schemes for distributed solar collector fields. Part II: Advanced control approaches. Solar Energy, 2007, Vol. 81, p. 1252-1272.
[7] Stuetzle T, Blair N, Mitchell JW, Beckman WA. Automatic control of a 30 MWe SEGS VI parabolic trough plant. Solar Energy, 2004, Vol. 76, p. 187-193.
[8] Relloso S, Lata J. Molten salt thermal storage: a proven solution to increase plant dispatchability. Experience in Gemasolar power plant. Proceedings of 17th SolarPACES Symposium, Granada, Spain, 2011.
[9] Wagner MJ, Zhu G. A generic CSP performance model for NREL's System Advisor Model. Proceedings of 17th SolarPACES Symposium, Granada, Spain, 2011.
[10] Giuliano S, Buck R, Eguiguren S. Analysis of solar thermal power plants with thermal energy storage and solar hybrid operation strategy. Proceedings of 17th SolarPACES Symposium, Granada, Spain, 2011.
[11] Fisher U. et al. Gas turbine "solarization" – Modifications for solar/fuel hybrid operation. Solar Energy Engineering, 2004, Vol. 126, p. 872 – 878
[12] Garcia P. Codes for solar flux calculation dedicated to central receiver system applications. PhD thesis, 2007, University of Perpignan, France.
[13] Grange M. Modeling and design of a pressurized air solar receiver for the PEGASE project. PhD thesis, 2012, University of Perpignan, France.
[14] Vrinat M. Development of a high temperature air solar receiver based on compact heat exchanger technology. PhD thesis, 2010, University of Perpignan, France.
[15] Kays WM, London AL. Compact heat exchangers. 2nd edition, New York: McGraw-Hill Book Co., 1964